Acta Pharmacologica Sinica

www.nature.com/aps

ARTICLE

# DL0410 ameliorates cognitive disorder in SAMP8 mice by promoting mitochondrial dynamics and the NMDAR-CREB-BDNF pathway

Wen-wen Lian[1,2], Wei Zhou[1], Bao-yue Zhang[1], Hao Jia[1], Lv-jie Xu[1], Ai-lin Liu[1] and Guan-hua Du[1]

Alzheimer's disease (AD) is a worldwide problem and there are no effective drugs for AD treatment. Previous studies show that DL0410 is a multi-target, anti-AD agent. In this study, we investigated the therapeutic effect of DL0410 and its action mechanism in SAMP8 mice. DL0410 (1−10 mg·kg$^{-1}$·d$^{-1}$) was orally administered to 8-month-old SAMP mice (SAMP8) for 8 weeks. We showed that DL0410 administration effectively ameliorated the cognitive deficits in the Morris water maze test, novel object recognition test, and nest building test. We revealed that DL0410 dose-dependently increased the expression levels of the mitochondrial proteins (PGC-1α, Mitofusin 2, OPA1, and Drp1), and subsequently ameliorated the processes of mitochondrial biosynthesis, fusion, and fission in the cortex and hippocampus of SAMP8 mice. Furthermore, DL0410 administration promoted the expression of synaptic proteins (synaptophysin and PSD95) in the brain of SAMP8 mice, and upregulated the protein phosphorylation in NMDAR-CAMKII/CAMKIV-CREB pathway responsible for the synaptic plasticity. DL0410 administration dose-dependently increased the expression of BDNF and TrkB, and the neurotrophic effect was mediated via the ERK1/2 and PI3K-AKT-GSK-3β pathways. DL0410 administration upregulated Bcl-2, increased the Bcl-2/Bax ratio and the level of caspase 3 and PARP-1, alleviating neuronal apoptosis. We proposed that the NMDAR-CREB-BDNF pathway might establish a positive feedback loop between synaptic plasticity and neurotrophy, with CREB at the center. In summary, DL0410 promotes synaptic function and neuronal survival, thus ameliorating cognitive deficits in SAMP8 mice via improved mitochondrial dynamics and increased activity of the NMDAR-CREB-BDNF pathway. DL0410 is a promising candidate to treat aging-related AD, and deserves more research and development in future.

**Keywords:** DL0410; synapse plasticity; neurotrophy; mitochondrial dynamics; CREB

*Acta Pharmacologica Sinica* (2021) 42:1055–1068; https://doi.org/10.1038/s41401-020-00506-2

## INTRODUCTION

Alzheimer's disease (AD), the most common form of dementia in elderly people, is characterized by impaired learning and memory. The prevalence of AD continues to increase in China and worldwide, which makes it one of the greatest health challenges in the 21st century [1]. Neuropathologically, AD is characterized by progressive and irreversible degeneration in the brain along with aging and involves amyloid plaques, neurofibrillary tangles, neuron and synapse loss, neuroinflammation, and brain atrophy [2]. Although many studies have examined the pathology of AD and attempted to develop effective agents, there are still no curative drugs available to stop or reverse the effects of AD [3]. Considering the multiple factors involved AD, there is a growing consensus that drugs with multiple targets will probably be effective in defeating AD [4].

DL0410 (Fig. 1) was first found to be a potent inhibitor against acetylcholinesterase (AChE) and was subsequently shown to inhibit butylcholinesterase (BuChE) as well as antagonize the histidine 3 receptor (H3R) [5–7]. The therapeutic effect of DL0410 on amnesia has been verified in a series of AD-related animal models, including scopolamine-[8], *D*-galactose-[9], and $A\beta_{1-42}$-induced model mice [10] and APP/PS1 transgene mice [11, 12]. DL0410 showed a beneficial effect on cognitive defects and was equivalent to or better than the positive references donepezil and memantine. Several mechanisms of DL0410, such as AChE inhibition, reduced Aβ generation, protection of mitochondrial respiration, and inhibition of oxidative stress and neuroinflammation, have been identified. However, the key mechanism of DL0410 has not been clarified. As a potential anti-AD agent with multiple targets, DL0410 should be further investigated to verify its pharmacologic effect in various animal models of AD and to further explore its key targets or pathways.

SAMP8 mice exhibit typical features of accelerated aging, with a short life span and age-related learning and memory deficits [13, 14]. In addition, SAMP8 mice show key neuropathological features of AD, such as increased Aβ, abnormal phosphorylation of Tau, neuronal loss, mitochondrial disorder, and oxidative stress, which resemble those of AD patients [15]. Therefore, SAMP8 mice are proposed to be a classical model for sporadic AD and have been used to characterize memory-enhancing compounds in a series of studies.

Mitochondria are an energy factory for the physiological activities of cells, such as neurotransmitter release, ion channel

[1]State Key Laboratory of Bioactive Substance and Function of Natural Medicines, Institute of Materia Medica, Chinese Academy of Medical Sciences and Peking Union Medical College, Beijing 100050, China and [2]Department of Pharmacy, China-Japan Friendship Hospital, Beijing 100029, China
Correspondence: Ai-lin Liu (liuailin@imm.ac.cn) or Guan-hua Du (dugh@imm.ac.cn)

Received: 3 April 2020 Accepted: 6 August 2020
Published online: 31 August 2020

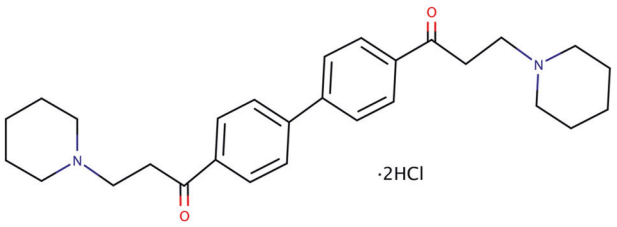


**Fig. 1 The chemical structure of DL0410.** DL0410 is the active compound with multiple drug targets against AD.

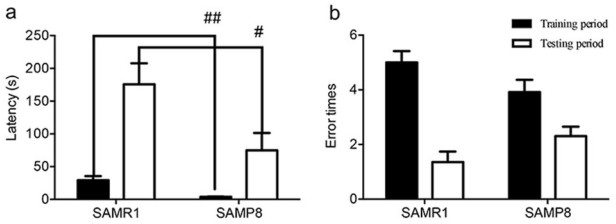


**Fig. 2 There was cognitive impairment in the 8-month-old SAMP8 mice compared with the SAMR1 mice in the step-down test.** Data are expressed as the mean±SEM ($n = 14$–15). **a** The latency of the SAMP8 mice was shorter than that of the SAMR1 mice, and **b** the error times of SAMP8 mice tended to increase. $^{\#}P < 0.05$ and $^{\#\#}P < 0.01$ vs the SAMR1 mice.

activity, and action potentials [16]. Mitochondrial injury can be caused by many factors, such as Aβ, oxidative stress, and nutritional deficits. When mitochondria are damaged, they can affect synaptic signaling and initiate and amplify cell apoptosis [17]. Synaptic disorder and neuron loss, which might result from mitochondrial disorder, nutrient deficiency, oxidative stress, and neuroinflammation, are the final injuries in AD pathology and further exacerbate the cognitive decline. Previously, DL0410 was found to improve mitochondrial respiration, as well as ameliorate neuron and synapse loss in *D*-galactose-induced aging mice [9]. However, the detailed mechanisms of DL0410 need to be determined further.

In the present study, we first assessed the therapeutic effect of DL0410 on SAMP8 mice, further explored its molecular mechanism from the aspect of synaptic function, neurotrophy and mitochondrial dynamics, and finally identified several key molecules and revealed a positive loop in the treatment of AD. This study suggests that DL0410 can be used in aging-related dementia and lays a foundation for its development in the future.

## MATERIALS AND METHODS

### Drugs and reagents

DL0410 (purity ≥ 98% by High-Performance Liquid Chromatography (HPLC)) was obtained from the Institute of Materia Medica, Chinese Academy of Medical Sciences (Beijing, China). Donepezil was obtained from Shandong Ji-nan Dexinjia Biotechnology (Ji-nan, China). RIPA (#9806) and primary antibodies against Bax (#14796), Bcl-2 (#3498), Caspase 3 (#9662), p-CREB (#9198), p-CAMKIIα (#3361), p-ERK1/2 (#4370), PI3K p110α (#4249), p-PI3K p85 (#4228), p-AKT (#9271), and p-GSK-3β (#5558) were purchased from Cell Signaling Technology (Danvers, MA, USA). Primary antibodies against Synaptophysin (ab32127), PSD95 (ab18258), p-CAMKIV (ab59424), BDNF (ab108319), TrkB (ab18987), PGC-1α (ab54481), Drp1 (ab184247), OPA1 (ab157457), and Mitofusin 2 (ab56889) were purchased from Abcam (Cambridge, UK). The primary antibodies against p-NMDAR2B (07-398) were purchased from Millipore (Billerica, MA, USA). Primary antibodies against poly (ADP-ribose) polymerase 1 (PARP-1, sc7150) were purchased from Santa Cruz (Santa Cruz, CA, USA). Primary antibodies against β-actin (30101ES60) were purchased from Yesen Biotechnology (Shanghai, China). A protease inhibitor cocktail (CW2200S), phosphatase inhibitor cocktail (CW2383S), bicinchoninic acid (BCA) protein assay kit (CW0014S), horseradish peroxidase (HRP)-conjugated secondary antibodies (anti-rabbit CW0234S, anti-mouse CW0221S), and ChemiGlow Western Blotting Detection Reagents (CW0049M) were purchased from Kangwei Biotechnology (Beijing, China).

### Animals and treatments

Three-month-old male SAMP8 and SAMR1 mice (18–20 g) were purchased from the laboratory animal center of the Peking University Health Science Center (Beijing, China). All mice were raised in the animal center of the Institute of Materia Medica, with a temperature of 23 ± 1 °C and humidity of 50% ± 10%. Mice had free access to food and water under a controlled 12 h light-dark cycle. The treatment and maintenance of the animals were in accordance with the *Guide for Care and Use of Laboratory Animals* (National Institutes of Health, Bethesda, MD, USA) and approved by the Animal Care Committee of the Institute of Materia Medica, Peking Union Medical College (Beijing, China).

When mice were 8 months old, 97 SAMP8 mice were used. These SAMP8 mice were randomly divided into five groups: the model group (SAMP8 group, 19 mice), the DL0410-1 mg/kg group (DL-1 group, 19 mice), the DL0410-3 mg/kg group (DL-3 group, 19 mice), the DL0410-10 mg/kg group (DL-10 group, 20 mice), and the donepezil group (20 mice). In addition, SAMR1 mice were set as the control group as described previously [18, 19]. All experiments were in accordance with the ARRIVE guidelines for Animal Research. A step-down test was used to evaluate the cognition of 14 SAMR1 mice and 15 SAMP8 mice. For this test, three SAMP8 mice were randomly selected from the five groups. In the testing period of the step-down test, the latency of the SAMP8 mice was significantly shorter than that of the SAMR1 mice (Fig. 2a), and the error times tended to increase (Fig. 2b). This result suggested that the memory and cognition of the 8-month-old SAMP8 mice were significantly impaired compared with that of the SAMR1 mice of the same age.

Mice were given drugs or water by intragastric gavage for 8 weeks. Mice in the control and model groups were given water. Mice in the donepezil, DL-1, DL-3, and DL-10 groups were administered donepezil at 3 mg/kg, DL0410 at 1 mg/kg, DL0410 at 3 mg/kg, and DL0410 at 10 mg/kg, respectively. DL0410 and donepezil were dissolved in distilled water. Eight weeks later, behavioral tests were conducted, and all of the tests were performed 30–40 min after drug administration.

### Behavioral tests

*Autonomous activity test*. This test was conducted in a round apparatus with six infrared detectors. When the mouse moved in the box, detectors could detect the signal and record it as "1". Mice were placed in the box with 1 min of adaption, and then, autonomous activity was recorded for 5 min. The autonomous activity was defined as the accumulation of the detected signals in 5 min.

*Morris water maze test*. The apparatus is composed of a circular pool (diameter 120 cm, height 40 cm) and a platform (diameter 8 cm, height 20 cm) in the center of the first quadrant. Water in the pool was 1 cm higher than that in the platform, which could not be seen by mice. The Morris water maze test lasted for 5 days; navigation trials were conducted on the first four days and the probe trial was conducted on the last day.

In the navigation trial, mice were first placed in the water in the middle of the second quadrant's border and then in the middle of the third quadrant's border. Mice were made to swim for 60 s each time. If they found the platform and stopped on it within 60 s, the recording system would stop, and the mice were allowed to stay

on the platform for 15 s to consolidate the memory. If not, the mice were guided to the platform and placed on it for 15 s.

In the probe trial, the platform was removed from the pool, and the mice were allowed to swim for 60 s two times. The position was the same as that in the navigation trial.

In the Morris water maze test, the swimming paths and times were recorded and used to analyze the space memory of the mice [9].

*Step-down test*. This test was conducted in an apparatus with a metal floor connected to electricity (36 V, 1.5 mA) and an insulated columnar platform on the floor. This test consisted of two phases: a training period (the first day) and a testing period (the second day).

On the first day, mice were placed into the apparatus for 1 min of adaptation and then placed on the platform after the power was on. In this 5 min training period, mice would step down to the floor and suffer an electric shock, which would force them to climb onto the platform to avoid the electric shock. On the second day, the mice were placed on the platform with power on, and the test lasted for 5 min.

In this test, latency (the time a mouse first stepped down to the metal floor) and error times (total number of times a mouse stepped down to the floor) were recorded [8].

*Novel object recognition test*. This test was conducted in a box (50 cm × 50 cm × 40 cm) with two objects in it. On the first day, mice were placed into the box without objects to adapt to the environment for 5 min. On the second day, two red cubes (4 cm × 4 cm × 4 cm) were placed in the box, 8 cm from the two nearest sides. Then, the mice were placed at the middle of the side far from objects and were recorded for 5 min. On the third day, one red cube was replaced by a blue cone, and then, the mice were placed in the box and recorded for 5 min.

In the recording period, the time mice spent exploring each object with their noses or paws was calculated. The discrimination index (DI) was further calculated to evaluate the curiosity of the mice toward the new object. The DI was defined as the percentage of time spent on the novel object (the blue cone) to the total time spent on the two objects [10].

*Nest building test*. This test was conducted in the cage with two stacks of tissues (4 cm × 4 cm, 6 pieces per stack). Nest building results were scored at 2, 12, and 24 h, in accordance with the following rules [20–22]:

0, tissues were not touched at all;

1, tissues were scattered in the cage;

2, tissues were put together in corner, without being torn;

3, tissues were put together in corner, with part of the tissues torn;

4, most tissues were torn and piled up to successfully form a nest.

Preparation of brain tissue

Thirty minutes after drug administration, the mice were sacrificed, and the cortex and hippocampus were collected and stored at −80 °C.

The cortex and hippocampus were homogenized in RIPA buffer supplemented with a protease inhibitor and phosphatase inhibitor. After centrifugation at 12,000 × *g* for 30 min, the supernatant was collected and boiled with loading buffer for 10 min. The denatured protein was stored at −80 °C for Western blot analysis.

Western blotting

SDS-PAGE was used to separate protein samples (total protein 50 μg), which were then transferred to a PVDF membrane. After the membrane was blocked by 5% BSA, it was incubated with different primary antibodies [Bax (rabbit, 1:1000), Bcl-2 (rabbit, 1:1000), Caspase 3 (rabbit, 1:1000), p-CREB (rabbit, 1:1000), p-CAMKIIα (rabbit, 1:1000), p-ERK1/2 (rabbit, 1:1000), PI3K p110α (rabbit, 1:1000), p-PI3K p85 (rabbit, 1:1000), p-AKT (rabbit, 1:1000), p-GSK-3β (rabbit, 1:1000), synaptophysin (rabbit, 1:20000), PSD95 (rabbit, 1:800), p-CAMKIV (rabbit, 1:1000), BDNF (rabbit, 1:5000), TrkB (rabbit, 1:1000), PGC-1α (rabbit, 1:1000), Drp1 (rabbit, 1:1000), OPA1 (rabbit, 1:2000), Mitofusin 2 (mouse, 1:1000), and β-actin (mouse, 1:10000)] at 4 °C overnight. On the second day, the PVDF membrane was rinsed with TBST and then incubated with HRP-conjugated secondary antibody (anti-rabbit, 1:1000; anti-mouse, 1:5000) at 37 °C for 2 h. Protein bands were detected by an ECL kit using a ChemiDoc-It$^{TM}$ imaging system (UVP, Upland, CA, USA). β-Actin was selected as a control [16, 17], and the gray value was analyzed by Gel-pro 32 (Media Cybernetics, Rockville, MD, USA).

Immunohistochemistry (IHC) analysis

Three mice were selected randomly from each group and anesthetized. Then, perfusion was conducted with saline solution and 4% paraformaldehyde. The isolated brains were preserved in 4% paraformaldehyde overnight. Brains embedded in paraffin were cut into 5 μm pieces and used for IHC staining.

Slides were dewaxed with xylene and a graded series of ethanol solutions. Then, they were incubated with primary antibodies [synaptophysin (rabbit, 1:500), PSD95 (rabbit, 1:100)] at 4 °C overnight. On the second day, the slides were rinsed and then incubated with secondary antibody (anti-rabbit, 1:100) at room temperature for 1 h. They were further visualized with an Elite ABC kit (Vector, Burlingame, CA, USA). Hematoxylin was used for nuclear staining. Then, the slides were imaged at 200× magnification using a microscope.

Statistical analysis

Data are expressed as the mean ± standard error of the mean (SEM). Statistical analyses were conducted with GraphPad Prism software (San Diego, CA, USA). Data for the navigation trials of the Morris water maze test were analyzed with two-way ANOVA with repeated measures, with time and drug treatment as two factors. Differences between the SAMR1 group and the SAMP8 group were analyzed with Student's *t*-test, and differences among the SAMP8 group and the other four drug-administered groups were evaluated with one-way ANOVA followed by Dunnett's multiple comparisons test. $P < 0.05$ was considered significant.

## RESULTS

DL0410 ameliorated cognitive impairments in the SAMP8 mice in the behavioral tests

*DL0410 showed no effect on the locomotor activity of the SAMP8 mice*. Locomotor activity was evaluated to exclude the effect of the drugs on motor function. There were no significant differences among the six groups (Fig. 3a) in locomotor activity, which indicated that DL0410 and donepezil had no effect on locomotor activity.

*DL0410 increased the DI of the SAMP8 mice in the novel object recognition test*. After 2 days of adaptation to the environment with two red cubes, one of the red cubes was replaced by a blue cone, and the time the mice spent exploring each object with their noses or paws was recorded. The DI was further calculated to evaluate the curiosity of the mice toward the new object, as shown in Fig. 3b. The DI of the SAMP8 group was significantly lower than that of the SAMR1 group ($P < 0.001$). DL0410 increased the DI of the SAMP8 mice in a dose-dependent manner ($P < 0.05$ at 1 mg/kg, $P < 0.001$ at 3 and 10 mg/kg), and donepezil significantly increased the DI ($P < 0.05$).

*DL0410 improved the nesting score of the SAMP8 mice in the nest building test*. Nest building is an instinct of mice, which was used

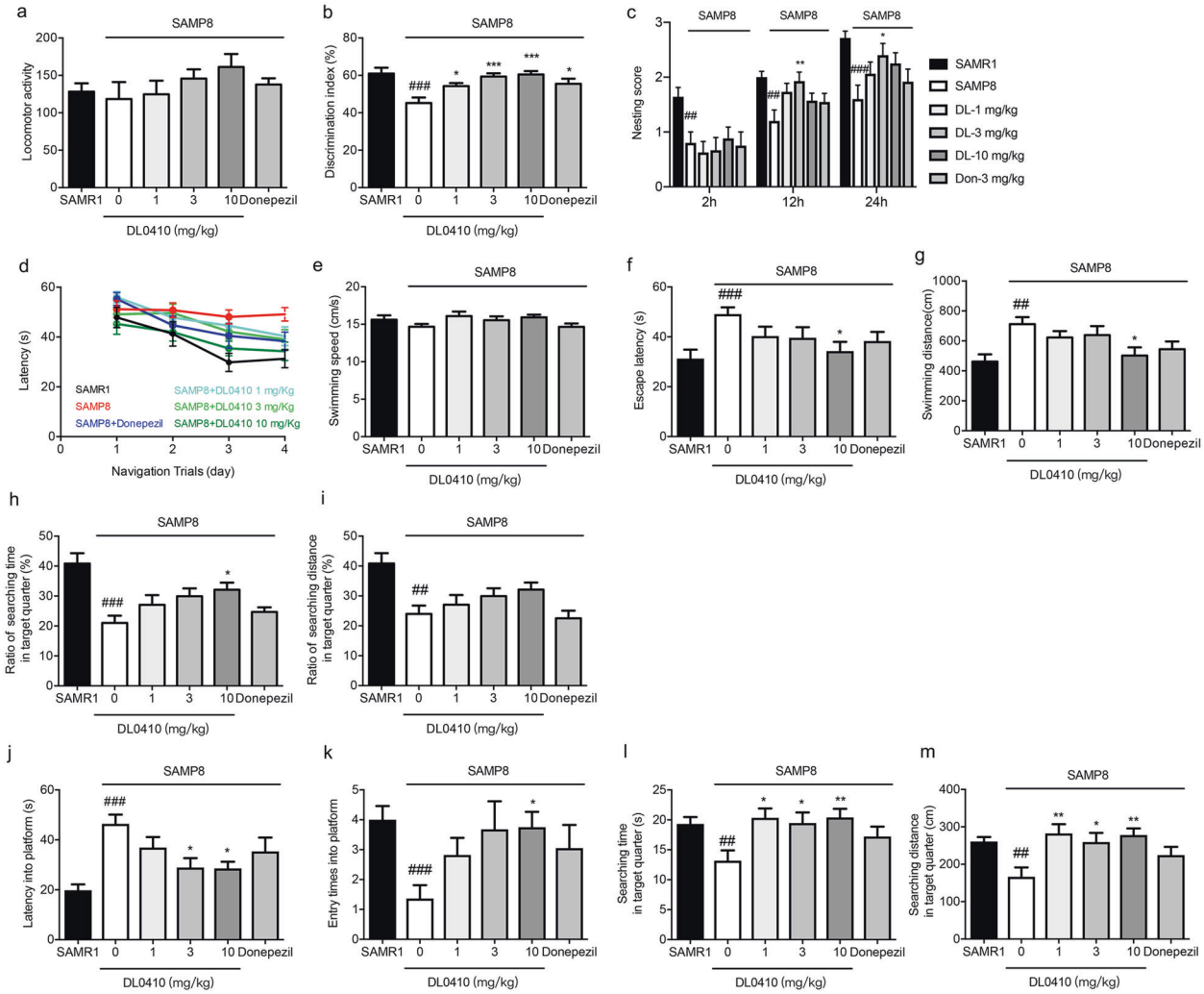


**Fig. 3 The effect of DL0410 on the memory of the SAMP8 mice in the behavioral tests.** Data are expressed as the mean±SEM ($n = 12–18$). The SAMP8 mice were randomly divided into 5 groups: the SAMP8 group (SAMP8+DL0410-0 mg/kg), DL-1 mg/kg group (SAMP8+DL0410-1 mg/kg), DL-3 mg/kg group (SAMP8+DL0410-3 mg/kg), DL-10 mg/kg group (SAMP8+DL0410-10 mg/kg), and donepezil group (SAMP8 +donepezil). SAMR1 mice were used as the control group. **a** There was no difference among the groups in locomotor activity. **b** DL0410 increased the DI of the SAMP8 mice in the novel object recognition test. **c** In the nest building test, DL0410 improved the nesting score of the SAMP8 mice at 12 and 24 h. In the navigation trials of the Morris water maze, the latency decreased as the training progressed (**d**). On the fourth day, there was no difference among the groups in the swimming speed (**e**); in addition, DL0410 shortened the latency (**f**) and swimming distance (**g**); in terms of searching strategy, DL0410 increased the ratio of searching time (**h**) and searching distance (**i**) in the target quarter. In the probe trial, DL0410 decreased the latency onto the platform (**j**) and increased the entry times onto the platform (**k**). In terms of searching strategy, DL0410 could increase the searching time (**l**) and distance (**m**) in the target quarter. $^{\#\#}P < 0.01$, $^{\#\#\#}P < 0.001$ vs the SAMR1 group; $^{*}P < 0.05$, $^{**}P < 0.01$, and $^{***}P < 0.001$ vs the SAMP8 group.

to explore the ability to complete daily tasks. The nest building results at 2, 12, and 24 h are shown in Fig. 3c. At 2 h, the score of the SAMP8 group was significantly lower than that of the SAMR1 group ($P < 0.01$), indicating that the SAMR1 mice started to build nests earlier than the SAMP8 mice. At 12 h, the score of the SAMP8 group was still lower than that of the SAMR1 group ($P < 0.01$), and DL0410 tended to increase the score of the SAMP8 mice, with the 3 mg/kg group showing significant results ($P < 0.01$). At 24 h, the scores of all the groups increased, and the nests built by the SAMR1 mice were three-dimensional and perfect. The score of the SAMP8 group was still lower than that of the SAMR1 group ($P < 0.001$), but treatment with DL0410 at 3 mg/kg significantly increased the score of the SAMP8 mice ($P < 0.05$). The SAMP8 mice treated with donepezil showed an increased trend in the nesting ability at 12 and 24 h, although the results were not significant.

*DL0410 improved the spatial memory of the SAMP8 mice in the Morris water maze test.* During the first four days, navigation trials were performed, and the results are shown in Fig. 3d–i. On the first day, the escape latency of each group was not significantly different. As the training progressed, the escape latency of the SAMR1 mice and the drug-administered SAMP8 mice tended to decrease, while the latency of the SAMP8 group almost never changed (Fig. 3d). The results of the fourth day were further analyzed, and there was no difference in the swimming speed among the groups (Fig. 3e); compared with those of the SAMR1 group, the escape latency and swimming distance of the SAMP8 group were significantly extended (Fig. 3f, g, $P < 0.001$ for escape latency, $P < 0.01$ for swimming distance). Treatment of the SAMP8 mice with DL0410 reduced the escape latency and swimming distance, with a significant difference at 10 mg/kg ($P < 0.05$ for both). The search strategy of the mice was further considered, and the ratio of searching time and distance in

the target quarter of the SAMP8 mice was increased by DL0410 (Fig. 3h, i), with 10 mg/kg notably increasing the ratio of searching time in the target quarter ($P < 0.05$).

On the fifth day, the platform was removed, and a probe trial was performed, with the results shown in Fig. 3j–m. Compared with those of the SAMR1 group, the latency onto the platform of the SAMP8 group was increased (Fig. 3j, $P < 0.001$), and the entry times onto the platform were reduced (Fig. 3k, $P < 0.001$). DL0410 decreased the latency onto the platform and increased the entry times onto the platform, with significant results observed in the 3 and 10 mg/kg groups (Fig. 3j for latency onto the platform, $P < 0.05$ at 3 and 10 mg/kg; Fig. 3k for entry times onto the platform, $P < 0.05$ at 10 mg/kg). With regard to the search strategy, DL0410 (1, 3 and 10 mg/kg) notably increased the searching time and distance in the target quarter (Fig. 3l for searching time in the target quarter, $P < 0.05$ at 1 and 3 mg/kg, $P < 0.01$ at 10 mg/kg; Fig. 3m for searching distance in the target quarter, $P < 0.01$ at 1 and 10 mg/kg, $P < 0.05$ at 3 mg/kg). Donepezil only showed a trend of improvement in the spatial memory of the SAMP8 mice in the navigation and probe trials.

## DL0410 ameliorated mitochondrial dynamics in the brains of the SAMP8 mice

Brains are highly dependent on energy, and mitochondrial function is extremely important for the physiological functions of neurons, such as synaptic transduction. We next determined the effect of DL0410 on mitochondria based on mitochondrial biosynthesis, fission and fusion.

*DL0410 improved the expression of PGC-1α in the brains of the SAMP8 mice*. PGC-1α is a transcriptional coactivator that participates in regulating the expression of energy metabolism-related genes and is involved in oxidative phosphorylation and mitochondrial integrity. As shown in Fig. 4a, the expression of PGC-1α in the SAMP8 group was notably downregulated compared with that of the SAMR1 group ($P < 0.01$ in the cortex, $P < 0.001$ in the hippocampus). In addition, DL0410 upregulated PGC-1α expression in the SAMP8 mice ($P < 0.01$ at 10 mg/kg in the cortex; $P < 0.05$ at 1 and 3 mg/kg, $P < 0.001$ at 10 mg/kg in the hippocampus).

*DL0410 increased the expression of Drp1 in the brains of the SAMP8 mice*. Drp1 is a key protein in mitochondrial fission, as shown in Fig. 4b. Drp1 expression was significantly lower in the cortex and hippocampus of the SAMP8 group than in the SAMR1 group ($P < 0.001$ in the cortex and hippocampus). DL0410 at 10 mg/kg rescued Drp1 expression in the SAMP8 mice ($P < 0.05$ in the cortex and hippocampus).

*DL0410 upregulated Mitofusin 2 and OPA1 in the brains of the SAMP8 mice*. Mitofusin 2 and OPA1, two key molecules in mitochondrial fusion, were investigated, and the results are shown in Fig. 4c–e. The levels of Mitofusin 2 and OPA1 in the cortex and hippocampus were lower in the SAMP8 group than in the SAMR1 group (for Mitofusin 2: $P < 0.001$ in the cortex and hippocampus; for OPA1: $P < 0.001$ in the cortex and hippocampus). Moreover, DL0410 treatment significantly promoted the expression of Mitofusin 2 and OPA1 in the cortex and hippocampus of the SAMP8 mice (for Mitofusin 2: $P < 0.05$ at 10 mg/kg in the cortex, $P < 0.01$ at 1 and 10 mg/kg, $P < 0.05$ at 3 mg/kg in the hippocampus; for OPA1: $P < 0.01$ at 10 mg/kg in the cortex, $P < 0.001$ at 1, 3 and 10 mg/kg in the hippocampus).

## The effect of DL0410 on synaptic plasticity in the brains of the SAMP8 mice

Synapses are the units involved in information transfer and storage, the structure and function of which can be altered based on the physiological situation. When synaptic plasticity is impaired, learning and memory are subsequently disordered. In this section, we investigated the expression of proteins involved in synaptic plasticity and the LTP-related signaling pathway.

*DL0410 promoted the expression of synaptic proteins in the brains of the SAMP8 mice*. Synaptophysin is specifically located in the presynaptic membrane and plays a key role in the release of neurotransmitters. As shown in Fig. 5c, the expression of synaptophysin showed no significant changes among the groups ($P > 0.05$). PSD95 is broadly expressed in the postsynaptic membranes of excitatory glutamatergic synapses. The expression of PSD95 was significantly decreased in the SAMP8 group compared with the SAMR1 group (Fig. 5f, $P < 0.01$ in the cortex, $P < 0.001$ in the hippocampus), which indicated that the postsynaptic density was damaged. However, the treatment of SAMP8 mice with DL0410 notably increased PSD95 expression in a dose-dependent manner ($P < 0.05$ at 10 mg/kg in the cortex; $P < 0.05$ at 1 and 3 mg/kg, $P < 0.001$ at 10 mg/kg in the hippocampus).

We further examined the expression of synaptophysin and PSD95 by immunohistochemical staining, with the results shown in Fig. 5a, b, d, and e. Synaptophysin and PSD95 in the cell and membrane were stained brown, and the IHC results were similar to the Western blot results. There was no obvious difference in the staining of synaptophysin among the six groups. However, the staining of PSD95 in the SAMP8 group was lighter than that of the SAMR1 group in the cortex and the hippocampal CA3 area. Moreover, the treatment of SAMP8 mice with DL0410 indeed promoted PSD95 expression.

*DL0410 promoted the NMDAR-CAMKII/IV-CREB pathway in LTP transduction*. LTP, an important part of synaptic function, participates in the learning and memory process. In the LTP cascade, NMDA receptor (NMDAR) mediates calcium influxes, CAMKII and CAMKIV are phosphorylated, and CREB is translocated into the nucleus. Thus, related proteins were investigated.

NMDAR2B (NR2B) is the regulatory subunit of the NMDAR, which is a voltage and neurotransmitter-gated ion channel involved in LTP. As shown in Fig. 6a, b, the phosphorylation of NR2B was significantly reduced in the SAMP8 group compared with the SAMR1 group ($P < 0.001$ in the cortex and hippocampus). Treatment with DL0410 increased the phosphorylation of NR2B in the cortex and hippocampus of the SAMP8 mice ($P < 0.01$ at 3 and 10 mg/kg in the cortex; $P < 0.01$ at 1 mg/kg, $P < 0.001$ at 3 and 10 mg/kg in the hippocampus).

CAMKII and CAMKIV are $Ca^{2+}$/Calmodulin-dependent protein kinases and participate in the early induction and late maintenance of LTP. As shown in Fig. 6a, c and d, the phosphorylation of CAMKII-α and CAMKIV was significantly lower in the SAMP8 group than in the SAMR1 group ($P < 0.001$ for p-CAMKII-α and p-CAMKIV in the cortex and hippocampus). In addition, DL0410 effectively improved the phosphorylation of CAMKII-α and CAMKIV in the cortex and hippocampus of the SAMP8 mice (Fig. 6c for p-CAMKII-α: $P < 0.05$ at 3 mg/kg, $P < 0.001$ at 10 mg/kg in the cortex; $P < 0.05$ at 1 mg/kg, $P < 0.01$ at 3 and 10 mg/kg in the hippocampus; Fig. 6d for p-CAMKIV: $P < 0.001$ at 10 mg/kg in the cortex; $P < 0.01$ at 1 and 3 mg/kg, $P < 0.001$ at 10 mg/kg in the hippocampus).

CREB is a vital nuclear translocation factor regulated by CAMK and controls the expression of numerous genes. The phosphorylation of CREB at Ser133 in the SAMP8 group was lower than that of the SAMR1 group in the cortex and hippocampus (Fig. 6a and e, $P < 0.001$ in the cortex and hippocampus). The administration of DL0410 facilitated the phosphorylation of CREB at Ser133 in the SAMP8 mice ($P < 0.05$ at 3 mg/kg, $P < 0.001$ at 10 mg/kg in the cortex; $P < 0.05$ at 3 mg/kg, $P < 0.01$ at 10 mg/kg in the hippocampus).

## DL0410 promoted the neurotrophic effect in the brains of the SAMP8 mice

BDNF is one of the neurotrophins widely distributed in the cortex and hippocampus and contributes to neuronal survival, synaptic

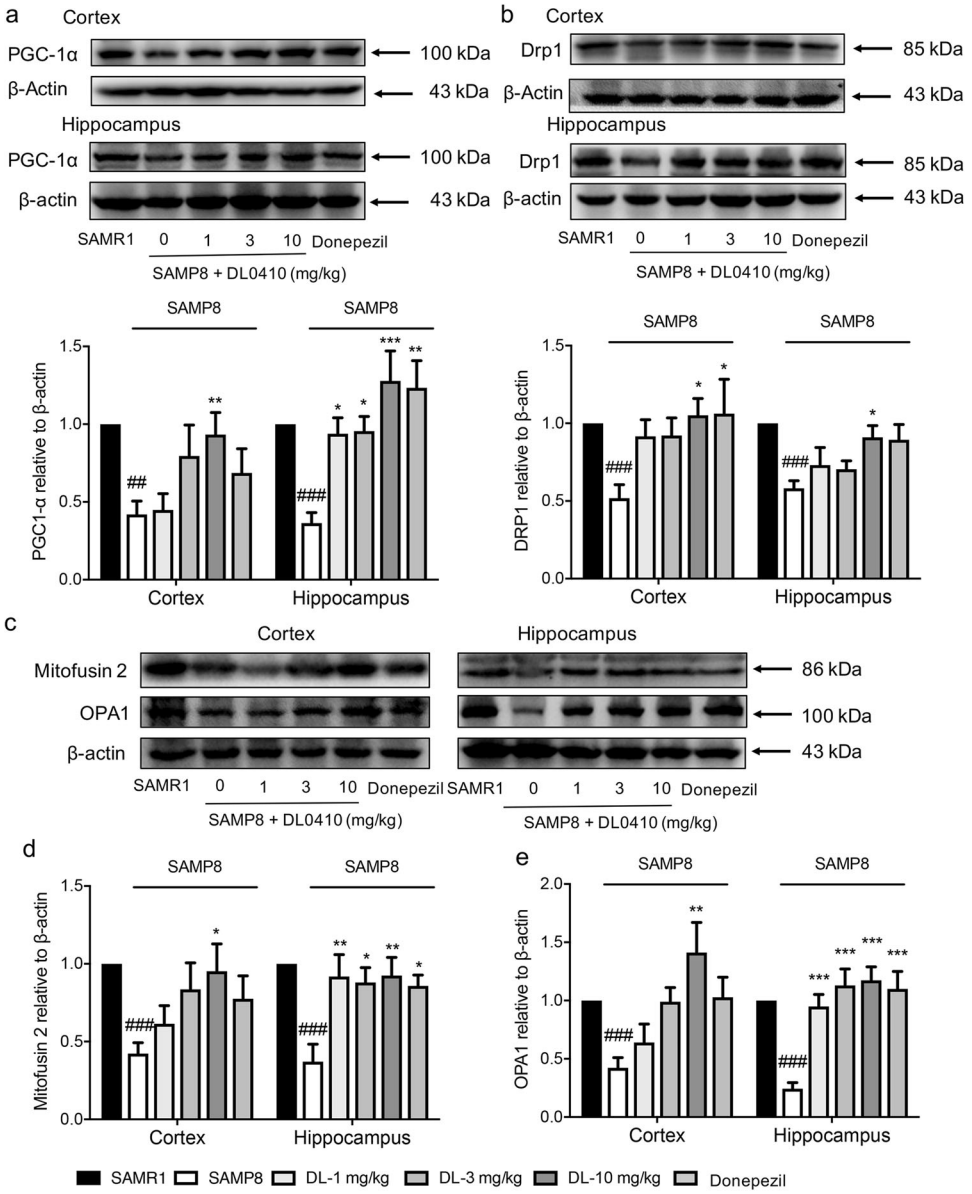


**Fig. 4 The effect of DL0410 on the mitochondrial protein in the brains of the SAMP8 mice.** Data are expressed as the mean±SEM ($n = 6–8$). DL0410 could improve the levels of PGC-1α (**a**), Drp1 (**b**), Mitofusin 2 (**d**) and OPA1 (**e**) in the cortex and hippocampus of the SAMP8 mice. **c** The representative bands of Mitofusin 2 and OPA1 in Western blots. SAMR1 mice were set as the control group, and SAMP8 mice were randomly divided into 5 groups: the SAMP8 group (SAMP8+DL0410-0 mg/kg), DL-1 mg/kg group (SAMP8+DL0410-1 mg/kg), DL-3 mg/kg group (SAMP8+DL0410-3 mg/kg), DL-10 mg/kg group (SAMP8+DL0410-10 mg/kg), and donepezil group (SAMP8+donepezil). In the histogram, the SAMR1 group, SAMP8 group, DL-1 mg/kg group, DL-3 mg/kg group, DL-10 mg/kg group, and donepezil group are listed from left to right. $^{\#\#}P < 0.01$ and $^{\#\#\#}P < 0.001$ vs the SAMR1 group; $^{*}P < 0.05$, $^{**}P < 0.01$, and $^{***}P < 0.001$ vs the SAMP8 group.

development and activity. In this section, we observed the BDNF-mediated signaling pathway.

*DL0410 increased the expression of BDNF and TrkB in the brains of the SAMP8 mice.* TrkB, the specific receptor of BDNF, mediates the neurotrophic effect by specific BDNF binding, and the analysis of this molecules is shown in Fig. 7a-c. Compared with those in the SAMR1 group, the levels of BDNF and TrkB were significantly decreased in the cortex and hippocampus of the SAMP8 group (for BDNF: $P < 0.001$ in the cortex and hippocampus; for TrkB: $P < 0.001$ in the cortex and hippocampus). Treatment with DL0410 increased the levels of BDNF and TrkB in the SAMP8 mice (Fig. 7b for BDNF: $P < 0.01$ at 3 mg/kg and $P < 0.001$ at 10 mg/kg in the cortex, $P < 0.05$ at 3 and 10 mg/kg in the hippocampus; Fig. 7c for TrkB: $P < 0.01$ at 10 mg/kg in the cortex, $P < 0.05$ at 3 mg/kg, and $P < 0.001$ at 10 mg/kg in the hippocampus).

*DL0410 increased p-ERK1/2 in the brains of the SAMP8 mice.* The MAPK pathway is activated by the binding of BDNF to TrkB, which further phosphorylates ERK1/2 and induces downstream pathways. The p-ERK1/2 results are shown in Fig. 7d. The phosphorylation of ERK1/2 was significantly reduced in the cortex and hippocampus of the SAMP8 group compared with that in the SAMR1 group ($P < 0.01$ in the cortex, $P < 0.05$ in the hippocampus), although there were no significant differences in the cortex. Treatment of the SAMP8 mice with DL0410 notably raised the level of p-ERK1/2 in the cortex and hippocampus ($P < 0.05$ at 10 mg/kg in the cortex, $P < 0.001$ at 10 mg/kg in the hippocampus).

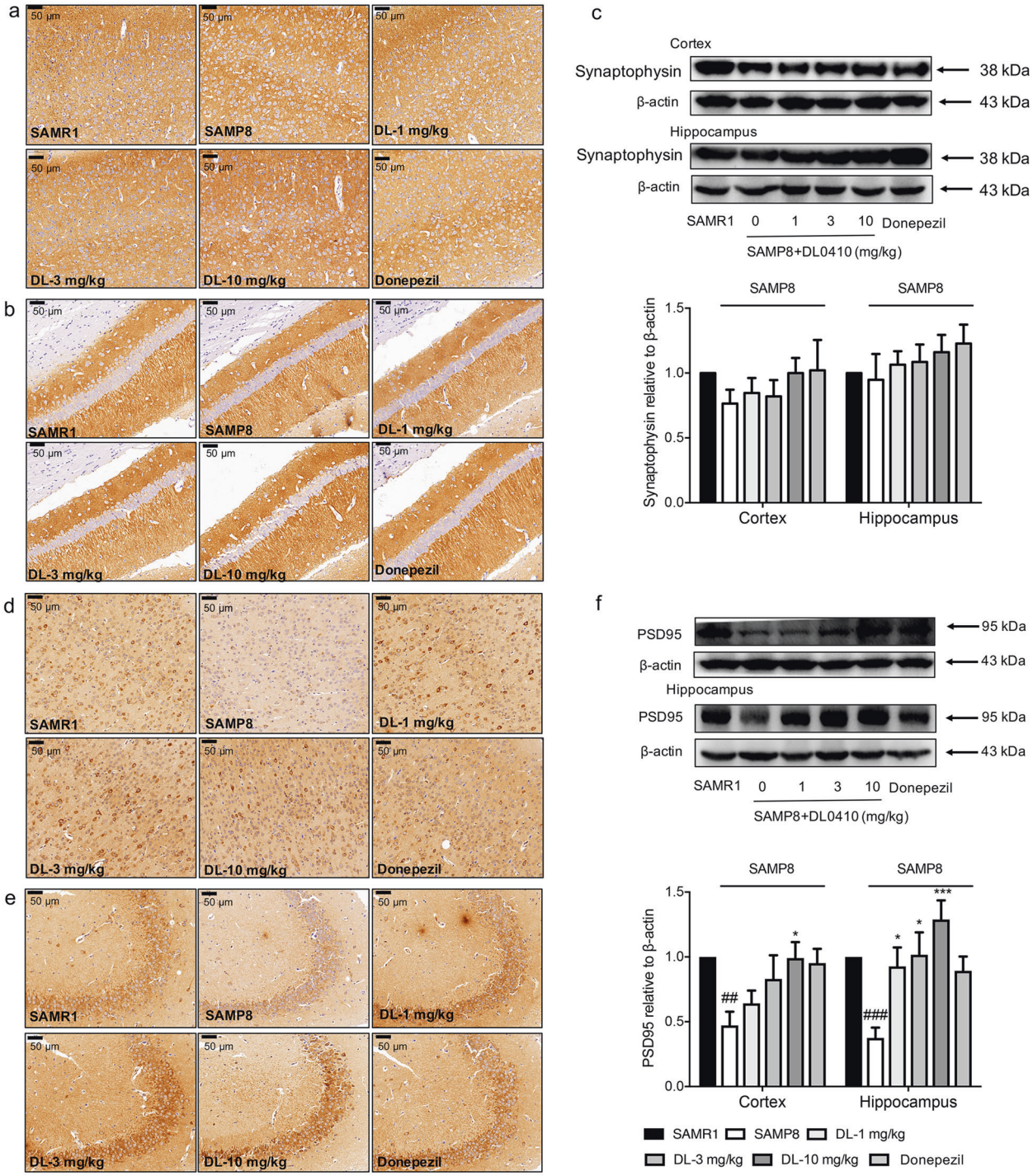


**Fig. 5 The effect of DL0410 on synaptic proteins in the brains of the SAMP8 mice.** Data are expressed as the mean±SEM ($n = 6–8$). The IHC results of synaptophysin in the cortex (**a**, 200×) and CA1 area (**b**, 200×) and the Western blot results (**c**) are shown; DL0410 showed a tendency to increase synaptophysin expression in the cortex and hippocampus of the SAMP8 mice. DL0410 increased PSD95 expression in the SAMP8 mice, as shown by Western blots (**f**), and IHC of the cortex (**d**, 200×) and CA1 area (**e**, 200×) showed similar results. SAMR1 mice were set as the control group, and SAMP8 mice were randomly divided into 5 groups: the SAMP8 group (SAMP8+DL0410-0 mg/kg), DL-1 mg/kg group (SAMP8+DL0410-1 mg/kg), DL-3 mg/kg group (SAMP8+DL0410-3 mg/kg), DL-10 mg/kg group (SAMP8+DL0410-10 mg/kg), and donepezil group (SAMP8+donepezil). In the histogram, the SAMR1 group, SAMP8 group, DL-1 mg/kg group, DL-3 mg/kg group, DL-10 mg/kg group, and donepezil group are listed from left to right. $^{\#\#}P < 0.01$ and $^{\#\#\#}P < 0.001$ vs the SAMR1 group; $^{*}P < 0.05$ and $^{***}P < 0.001$ vs the SAMP8 group.

*DL0410 promoted the PI3K-AKT pathway in the brains of the SAMP8 mice.* The PI3K-AKT pathway is another important pathway activated by BDNF. PI3K is composed of the catalytic subunit p110 and the regulatory subunit p85, and the results are shown in Fig. 8a–c. The expression of p110α and p-p85 was significantly reduced in the cortex and hippocampus of the SAMP8 group compared with that of the SAMR1 group (for p110α: $P < 0.001$ in the cortex and hippocampus; for p-p85: $P < 0.001$ in the cortex and hippocampus). SAMP8 mice administered DL0410 at 10 mg/kg showed high levels of p110α and p-p85 in the cortex and

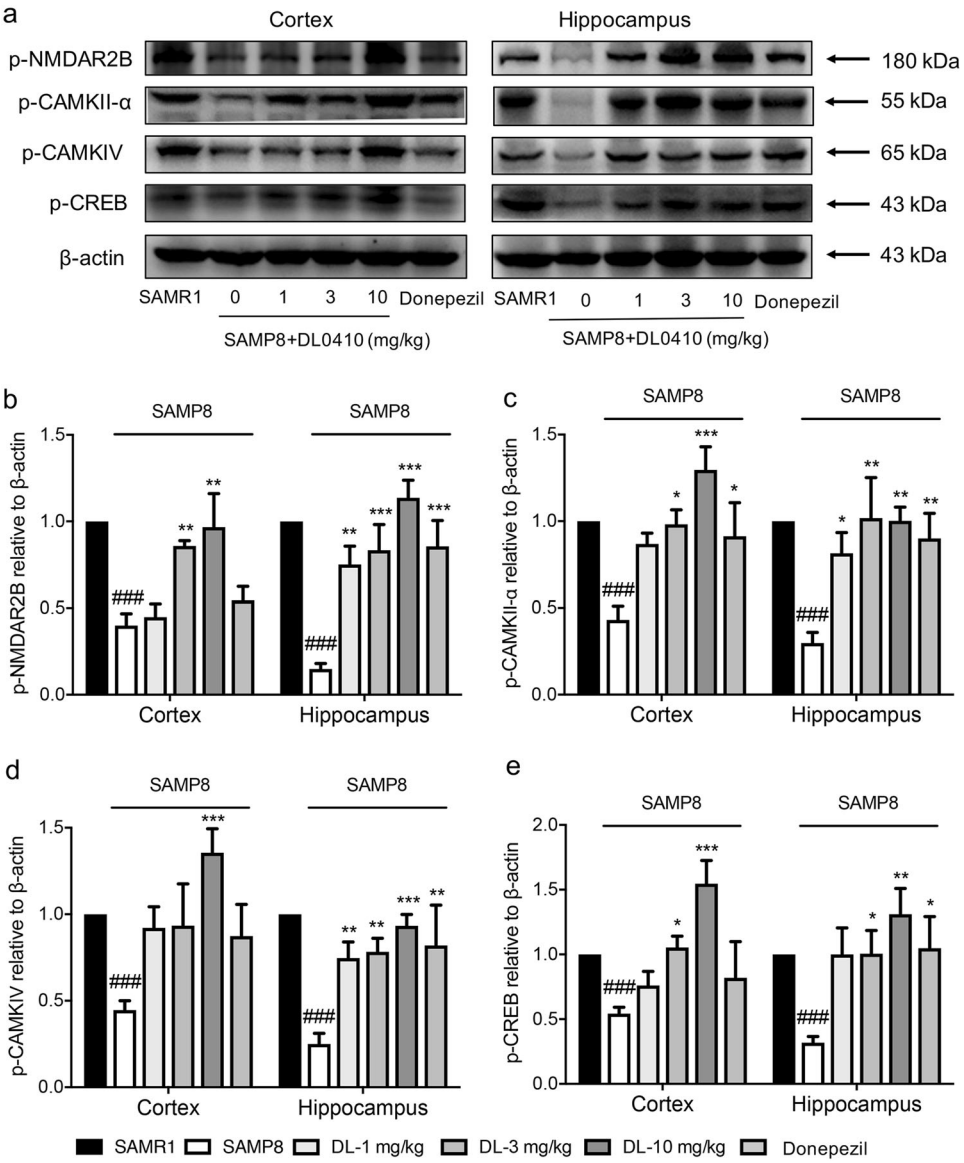


**Fig. 6 The effect of DL0410 on the expression of phosphorylated NMDAR2B, CAMKII-α, CAMKIV, and CREB in the brains of the SAMP8 mice.** Data are expressed as the mean ± SEM ($n = 6–8$). **a** Representative bands of Western blotting. DL0410 promoted the phosphorylation of NMDAR2B (**b**), CAMKII-α (**c**), CAMKIV (**d**) and CREB (**e**) in the cortex and hippocampus of the SAMP8 mice. SAMR1 mice were set as the control group, and SAMP8 mice were randomly divided into 5 groups: the SAMP8 group (SAMP8+DL0410-0 mg/kg), DL-1 mg/kg group (SAMP8+DL0410-1 mg/kg), DL-3 mg/kg group (SAMP8+DL0410-3 mg/kg), DL-10 mg/kg group (SAMP8+DL0410-10 mg/kg), and donepezil group (SAMP8+donepezil). In the histogram, the SAMR1 group, SAMP8 group, DL-1 mg/kg group, DL-3 mg/kg group, DL-10 mg/kg group and donepezil group are listed from left to right. $^{###}P < 0.001$ vs the SAMR1 group; $^{*}P < 0.05$, $^{**}P < 0.01$, and $^{***}P < 0.001$ vs the SAMP8 group.

hippocampus (Fig. 8b for p110α: $P < 0.05$ at 10 mg/kg in the cortex, $P < 0.01$ at 10 mg/kg in the hippocampus; Fig. 8c for p-p85: $P < 0.05$ at 10 mg/kg in the cortex, $P < 0.05$ at 1 and 3 mg/kg, $P < 0.01$ at 10 mg/kg in the hippocampus).

AKT and GSK-3β are downstream molecules of PI3K, which are further phosphorylated. As shown in Fig. 8a, d, and e, the levels of p-AKT and p-GSK-3β (Ser9) were significantly lower in the SAMP8 group than in the SAMR1 group (for p-AKT: $P < 0.001$ in the cortex and hippocampus; for p-GSK-3β (Ser9): $P < 0.001$ in the cortex and hippocampus). However, the treatment of SAMP8 mice with DL0410 increased the levels of p-AKT and p-GSK-3β (Ser9) compared with those of the SAMP8 group (Fig. 8d for p-AKT: $P < 0.01$ at 10 mg/kg in the cortex, $P < 0.05$ at 1 and 3 mg/kg, $P < 0.001$ at 10 mg/kg in the hippocampus; Fig. 8e for p-GSK-3β (Ser9): $P < 0.05$ at 10 mg/kg in the cortex, $P < 0.05$ at 1 mg/kg, $P < 0.01$ at 3 and 10 mg/kg in the hippocampus).

DL0410 alleviated neuronal apoptosis in the brains of the SAMP8 mice

One of the hallmarks of AD is neuron loss, which is the final result of different pathologies. In this section, we investigated the expression of apoptosis-related proteins.

Bcl-2 and Bax are located at the outer membrane of the mitochondria and inhibit and promote apoptosis, respectively. The ratio of Bcl-2 to Bax is decisive in the process of mitochondrial apoptosis. The Western blot results are shown in Fig. 9a, b. The expression of Bcl-2 was notably reduced in the cortex and hippocampus of the SAMP8 group compared with the SAMR1 group ($P < 0.001$ in the cortex and hippocampus). DL0410 increased Bcl-2 expression in the SAMP8 mice ($P < 0.001$ at 10 mg/kg in the cortex; $P < 0.05$ at 1, 3, and 10 mg/kg in the hippocampus) and further significantly increased the ratio of Bcl-2 to Bax at 10 mg/kg (Fig. 9c, $P < 0.05$ at 10 mg/kg in the hippocampus).

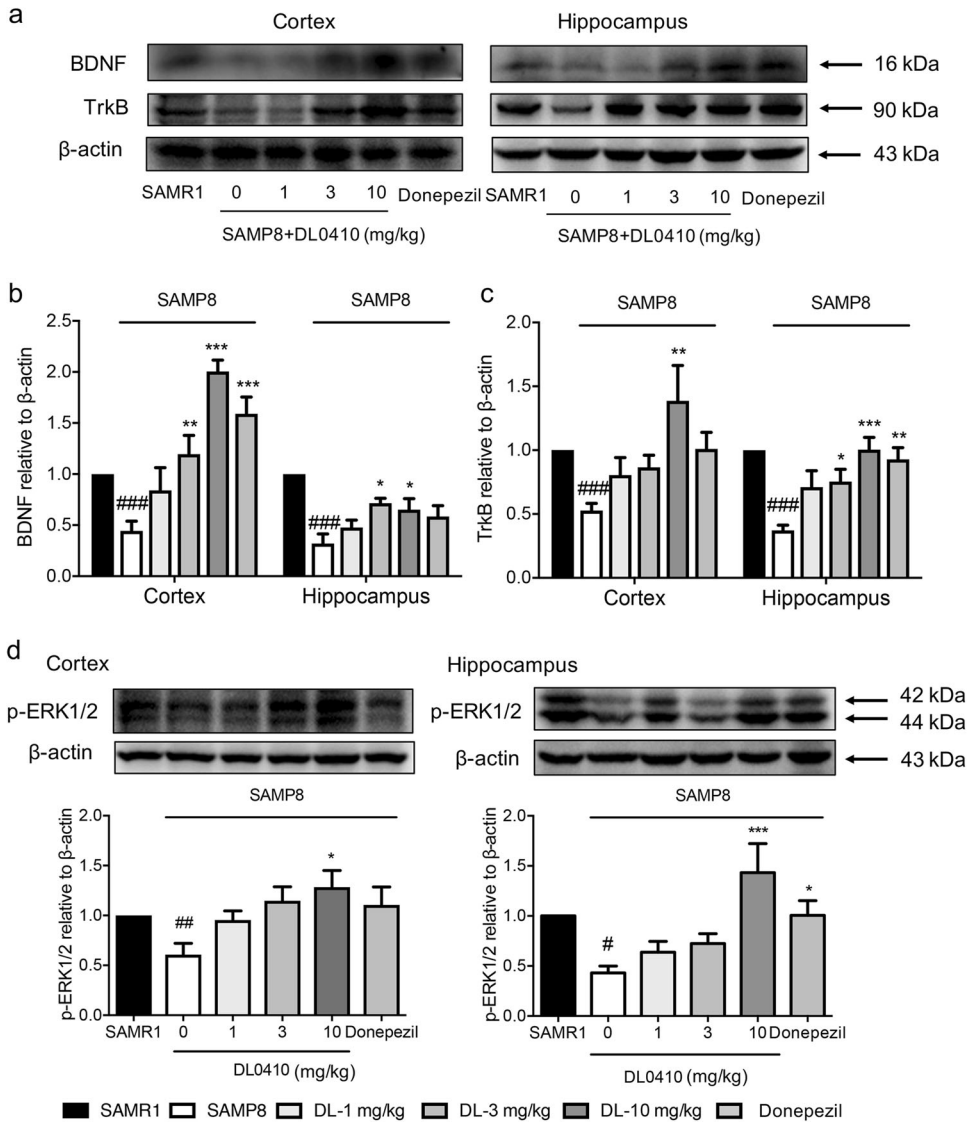


**Fig. 7 The effect of DL0410 on the expression of BDNF, TrkB, and phosphorylated ERK1/2 in the brains of the SAMP8 mice.** Data are expressed as the mean±SEM ($n = 6$–8). **a** Representative bands of Western blotting. DL0410 increased the levels of BDNF (**b**) and TrkB (**c**) and promoted the phosphorylation of ERK1/2 (**d**) in the cortex and hippocampus of the SAMP8 mice. SAMR1 mice were set as the control group, and SAMP8 mice were randomly divided into 5 groups: the SAMP8 group (SAMP8+DL0410-0 mg/kg), DL-1 mg/kg group (SAMP8+DL0410-1 mg/kg), DL-3 mg/kg group (SAMP8+DL0410-3 mg/kg), DL-10 mg/kg group (SAMP8+DL0410-10 mg/kg), and donepezil group (SAMP8 +donepezil). In the histogram, the SAMR1 group, SAMP8 group, DL-1 mg/kg group, DL-3 mg/kg group, DL-10 mg/kg group and donepezil group are listed from left to right. $^{\#}P < 0.05$, $^{\#\#}P < 0.01$, and $^{\#\#\#}P < 0.001$ vs the SAMR1 group; $^{*}P < 0.05$, $^{**}P < 0.01$, and $^{***}P < 0.001$ vs the SAMP8 group.

Caspase 3, an executor of apoptosis, is cleaved to the active form, which further cleaves and inactivates PARP-1. Compared with those in the SAMR1 group, Caspase 3 and PARP-1 were significantly reduced in the cortex and hippocampus in the SAMP8 group (Fig. 9a, d, e, $P < 0.001$ for Caspase 3 in the cortex and hippocampus; $P < 0.001$ for PARP-1 in the cortex and hippocampus). DL0410 increased the levels of Caspase 3 and PARP-1 in the SAMP8 mice (Fig. 9d for Caspase 3: $P < 0.05$ at 10 mg/kg in the cortex and hippocampus; Fig. 9e for PARP-1: $P < 0.05$ at 10 mg/kg in the cortex, $P < 0.05$ at 1 and 3 mg/kg, $P < 0.01$ at 10 mg/kg in the hippocampus). This result indicated that the cleavage of Caspase 3 and PARP-1 was suppressed, which inhibits apoptosis.

## DISCUSSION

In the present study, 8-month-old SAMP8 mice were used to study the therapeutic effect of DL0410 on cognitive deficits, with SAMR1 mice of the same age as controls. Moreover, the effect of DL0410 on mitochondrial dynamics, synaptic plasticity, neuronal apoptosis and neurotrophy was explored.

After 8 weeks of DL0410 administration, a series of behavioral tests were conducted to examine the learning and memory capabilities of the mice. In the autonomous activity test, there were no significant differences among the six groups, which implied that there was no difference in the motor ability of these mice. Therefore, the difference in results from the other tests is likely attributable to the different levels of learning and memory in each group. In the novel object recognition test, DL0410 raised the DI of the SAMP8 mice and increased the time the mice spent on the new object. In the nest building test, DL0410 could improve the ability to perform daily tasks and increased the ability to make nests, which significantly raised the scores at 12 and 24 h. The Morris water maze is a classic test of spatial memory, in which mice were tested on their ability to escape from the water

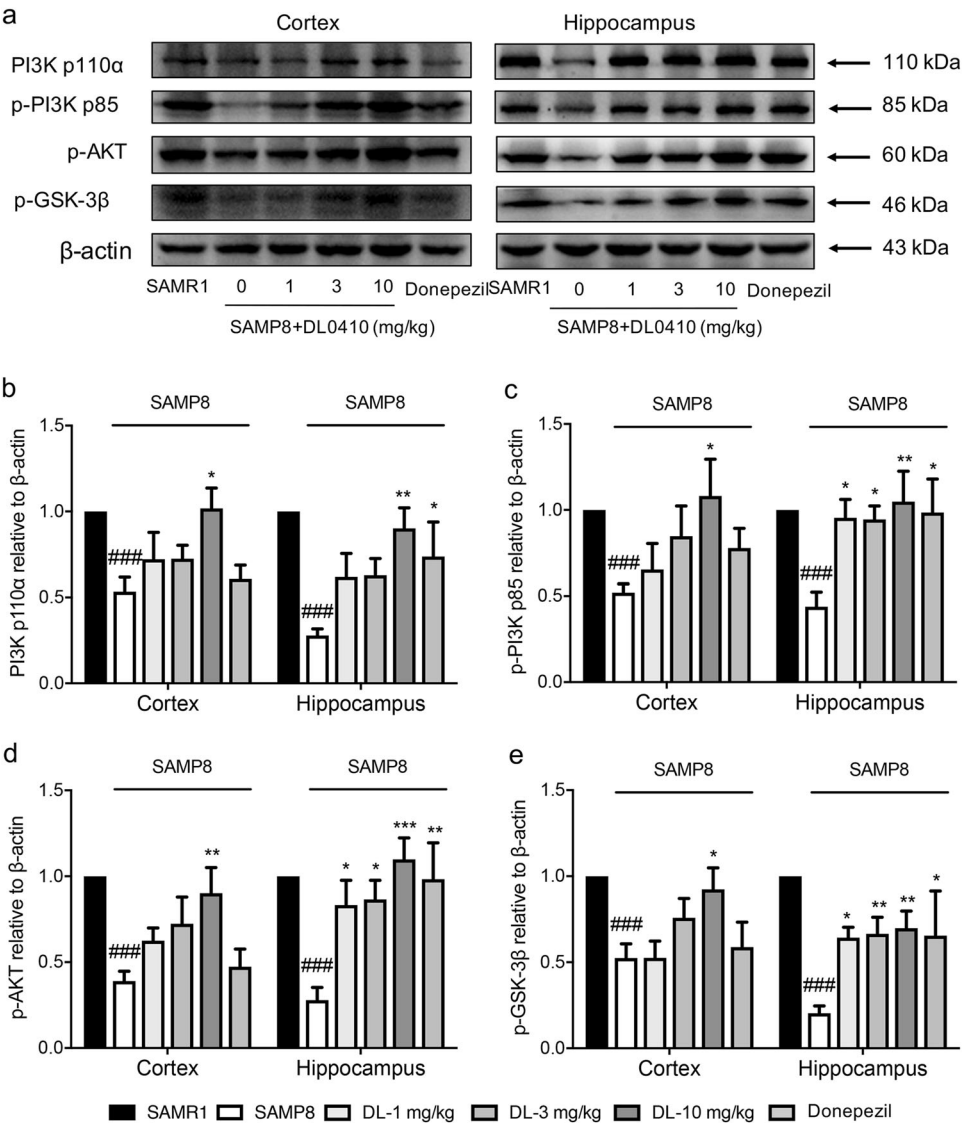


**Fig. 8 The effect of DL0410 on the PI3K-AKT-GSK-3β pathway in the brains of the SAMP8 mice.** Data are expressed as the mean±SEM ($n$ = 6–8). **a** Representative Western blot bands. DL0410 increased the expression of PI3K p110α (**b**) and the phosphorylation of PI3K p85 (**c**), AKT (**d**) and GSK-3β (Ser9) (**e**) in the cortex and hippocampus of the SAMP8 mice. SAMR1 mice were set as the control group, and SAMP8 mice were randomly divided into 5 groups: the SAMP8 group (SAMP8+DL0410-0 mg/kg), DL-1 mg/kg group (SAMP8+DL0410-1 mg/kg), DL-3 mg/kg group (SAMP8+DL0410-3 mg/kg), DL-10 mg/kg group (SAMP8+DL0410-10 mg/kg), and donepezil group (SAMP8+donepezil). In the histogram, the SAMR1 group, SAMP8 group, DL-1 mg/kg group, DL-3 mg/kg group, DL-10 mg/kg group and donepezil group are listed from left to right. $^{###}P < 0.001$ vs the SAMR1 group; $^{*}P < 0.05$, $^{**}P < 0.01$, and $^{***}P < 0.001$ vs the SAMP8 group.

according to environmental cues. On the fourth day of the navigation trials, the mice treated with DL0410 had decreased escape latencies and swimming distances and increased ratios of searching time in the target quarter. In the probe trial, DL0410 could effectively shorten the latency onto the platform, promote more entry times crossing the platform, and increase the searching time and distance in the target quarter. In summary, DL0410 dose-dependently ameliorated the performance of the SAMP8 mice in the behavioral tests, with 10 mg/kg being the most effective.

The quality and quantity of mitochondria are strictly controlled by dynamic biosynthesis, fission, and fusion. In biosynthesis, mitochondria are generated by proteins encoded by nuclear and mitochondrial DNA, which are regulated by PGC-1α. It has been reported that both PGC-1α mRNA and protein were reduced in AD patients [23] and in APP/PS1 and SAMP8 mice [24–27], indicating a deficit in mitochondrial biosynthesis during AD. Mitochondrial fission and fusion are vital processes that eliminate damaged mitochondria, exchange mtDNA and respiratory-related enzymes, maintain normal morphology and quantity, and send mitochondria to the axon terminal. Mitofusin 2 and OPA1, which participate in the fusion of the outer and inner membranes, were found to have low expression in the brains of AD patients with reduced ATP production [28]. When Mitofusin 2 was knocked out or OPA1 expression was inhibited, aberrant mitochondrial morphology with increased fragmentation was observed [29]. In 13-month-old APP/PS1 mice, increased Drp1 was found to interact with Aβ and phosphorylated Tau, which augmented Aβ toxicity in Manczak's study [30], while in Zhang's and Picca's studies, lower levels of Drp1 were found in 12-month-old APP/PS1 mice, and increased Drp1 could effectively ameliorate mitochondrial function and synaptic plasticity [29, 31]. The altered expression of Drp1 in APP/PS1 mice indicated the diversity of the functions of Drp1 during AD progression. Regardless of whether Drp1 is increased or decreased in APP/PS1 mice, the dynamic

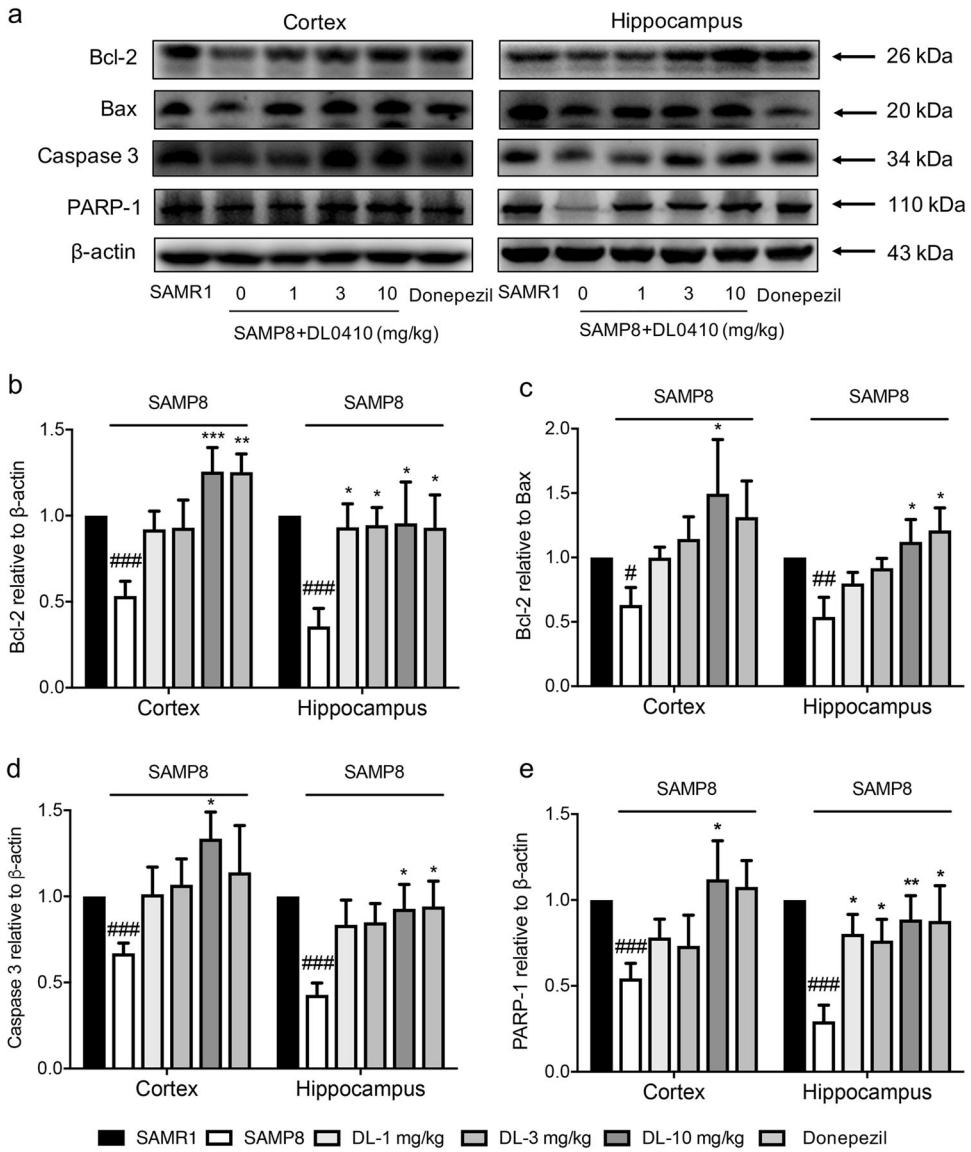


**Fig. 9 The effect of DL0410 on the apoptotic proteins in the brains of the SAMP8 mice.** Data are expressed as the mean ± SEM ($n = 6–8$). **a** Representative Western blot bands. DL0410 increased Bcl-2 expression (**b**) and raised the ratio of Bcl-2/Bax (**c**) in the cortex and hippocampus of the SAMP8 mice. The levels of Caspase 3 (**d**) and PARP-1 (**e**) induced by DL0410 were high in the cortex and hippocampus of the SAMP8 mice. SAMR1 mice were set as the control group, and SAMP8 mice were randomly divided into 5 groups: the SAMP8 group (SAMP8+DL0410-0 mg/kg), DL-1 mg/kg group (SAMP8+DL0410-1 mg/kg), DL-3 mg/kg group (SAMP8+DL0410-3 mg/kg), DL-10 mg/kg group (SAMP8+DL0410-10 mg/kg), and donepezil group (SAMP8+donepezil). In the histogram, the SAMR1 group, SAMP8 group, DL-1 mg/kg group, DL-3 mg/kg group, DL-10 mg/kg group and donepezil group are listed from left to right. $^{\#}P < 0.05$, $^{\#\#}P < 0.01$ and $^{\#\#\#}P < 0.001$ vs the SAMR1 group; $^{*}P < 0.05$, $^{**}P < 0.01$ and $^{***}P < 0.001$ vs the SAMP8 group.

equilibrium, normal morphology, and mitochondrial balance are adversely affected [32].

In the SAMP8 group, we found that PGC-1α, Mitofusin 2, OPA1 and Drp1 were expressed at lower levels than those in the SAMR1 mice. Widespread damage to mitochondrial dynamics might cause cells to die because of a lack of energy. However, DL0410 significantly reversed the expression of PGC-1α, Mitofusin 2, OPA1 and Drp1 in the brains of the SAMP8 mice and recovered mitochondrial biosynthesis, fusion and fission. Furthermore, the qualities and quantities of the mitochondria were acceptable, which enabled them to meet the energy requirements in different neuronal compartments in a timely manner.

The synapse is the basic unit participating in the transmission of the signal. In addition, the number, structure and degree of activity of synapses could change under different physical and pathological conditions, which is called synaptic plasticity [33, 34]. PSD95, a cytoskeletal protein in the postsynaptic density, is required for synapse formation and reception of synaptic stimuli [35]. This protein was reported to be reduced in the brains of AD patients and APP/PS1 and SAMP8 mice [36, 37]. The NMDA receptor, located in the postsynaptic density, is activated by neurotransmitters released from the presynaptic membrane, which further leads to the cascade of phosphorylation of its downstream molecules (CAMKII, CAMKIV, and CREB). The activation of the NMDA receptor and its downstream molecules are critical for the induction and maintenance of LTP. In addition, LTP inhibition in APP/PS1 and SAMP8 mice has been reported [37–39], and upregulated expression of NMDAR [40], CAMKII [41], CAMKIV [42], and CREB [39] could effectively ameliorate cognitive impairment.

In our study, DL0410 promoted the expression of PSD95, p-NR2B, p-CAMKIIα, p-CAMKIV, and p-CREB in the brains of the SAMP8 mice. Phosphorylated CAMKIIα and CAMKIV may lead to

the constant activation of NMDAR and CREB, which help maintain LTP and synapse plasticity [43].

BDNF is the most abundant neurotrophic factor in the brain and is widely expressed in fibroblasts, astrocytes and neurons. Moreover, BDNF is critical for long-term memory because it promotes neuron survival and synaptic plasticity. BDNF is regulated by CREB, which is dependent on synaptic activity; therefore, more BDNF is synthesized when synaptic activity increases [44–46]. TrkB, the specific receptor for BDNF, mediates the neurotrophic effect of BDNF via the PI3K-AKT, MAPK/ERK1/2 and PLCγ pathways [47, 48]. It has been reported that BDNF knockout mice showed LTP inhibition and memory deficits [49]. In addition, BDNF administration could recover LTP and memory in the BDNF-deficient mice, as well as in the control mice [47, 50, 51]. Moreover, BDNF-induced neurotrophy could stimulate the expression of synaptic proteins [52]. In TrkB knockout mice, the synaptic proteins PSD95 and LTP were suppressed, but overexpression of TrkB in mice enhanced the PLCγ pathway and memory ability [53, 54].

In the present study, lower levels of BDNF and TrkB were found in the cortex and hippocampus of the SAMP8 group than the SAMR1 group, which might result from impaired synaptic transmission. DL0410 treatment in the SAMP8 mice effectively increased the expression of BDNF and TrkB and further facilitated ERK1/2 and PI3K-AKT phosphorylation. GSK-3β is phosphorylated at Ser9 and inactivated, which helps to resist apoptosis [55]. CREB, which is a convergence point of the NMDAR-CAMKII/CAMKIV, ERK1/2, and PI3K-AKT pathways, regulated the expression of genes such as BDNF, Bcl-2, PSD95 and so on. Increased synaptic function can promote the expression of BDNF and Bcl-2, and BDNF in turn enhances synaptic plasticity and neuronal survival. The positive feedback loop of NMDAR-CREB-BDNF established by synaptic plasticity and neurotrophic effects was consolidated by DL0410 and played a critical role in recovering the learning and memory ability in the SAMP8 mice.

Neuronal loss can result from mitochondrial dynamic disorder or nutrient deficiency in AD through apoptosis, necrosis and pyroptosis [56]. The ratio of the antiapoptotic protein Bcl-2 to the proapoptotic protein Bax is key in initiating the mitochondrial apoptosis pathway [57–60]. Mitochondrial dynamics are also involved in apoptosis, with mitochondrial fragmentation preceding cytochrome *c* release and caspase activation. In the present study, Bcl-2 expression and the ratio of Bcl-2 to Bax were strikingly increased in the SAMP8 mice by DL0410, which inhibited the initiation of apoptosis in the mitochondrial pathway. We have demonstrated that DL0410 treatment could promote CREB phosphorylation via the NMDAR- and TrkB-mediated pathways and ameliorate mitochondrial dynamics in the SAMP8 mice. Therefore, the increased protein abundance of Bcl-2 in the DL0410-treated groups might be attributed to the high level of p-CREB and the enhanced mitochondrial function, and the ratio of Bcl-2/Bax further increased. In addition, decreases in Caspase 3 and PARP-1 cleavage were observed, which also prevented apoptosis of neurons.

In the present study, the mechanism of DL0410 was explored from the views of mitochondrial dynamics, synaptic plasticity, neurotrophy and neuronal apoptosis, with a detailed description in Fig. 10. DL0410 promoted the expression of PGC-1α, Drp1, OPA1 and mitofusin 2, which facilitate mitochondrial dynamics directly or indirectly. The postsynaptic pathway of NMDAR-CAMKII/CAMKIV-CREB was found to be enhanced by DL0410 to maintain LTP, and the neurotrophic effect of BDNF was improved via the ERK1/2 and PI3K-AKT-GSK-3β pathways. CREB, which is a downstream effector of these three pathways, further upregulated the expression of several genes, such as PSD95, BDNF, and Bcl-2, which promoted synaptic plasticity and neurotrophic effects and inhibited neuronal apoptosis. In addition, the NMDAR-CREB-BDNF pathway establishes a positive feedback loop, with CREB at the center. Well-balanced mitochondrial dynamics provide more energy for the NMDAR-mediated postsynaptic pathway and

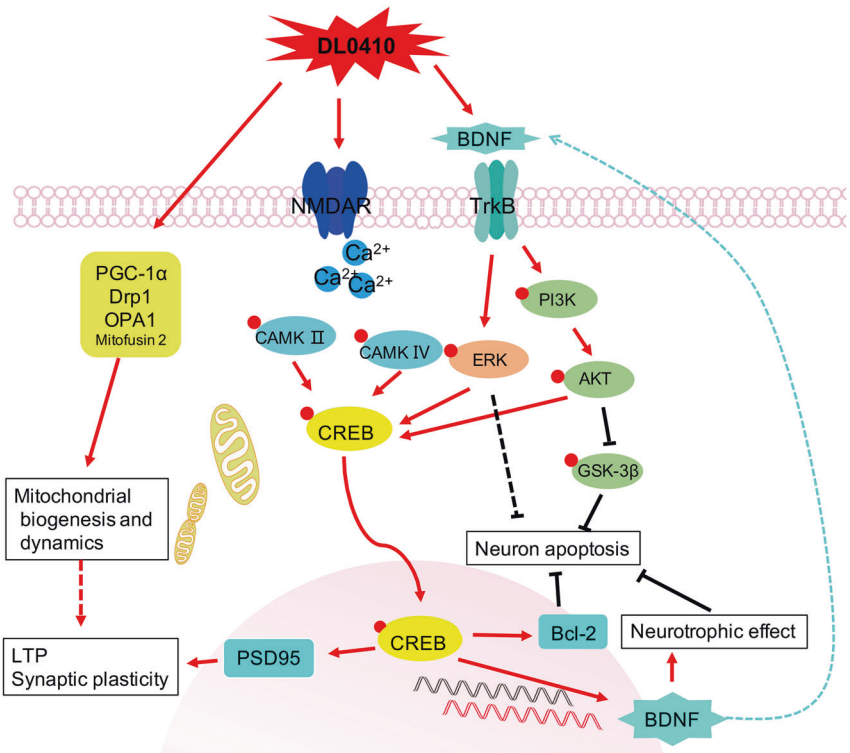


**Fig. 10 Illustration of the mechanism of DL0410.** The mechanism is related to mitochondrial dynamics, synaptic plasticity, neurotrophic effects and neuronal apoptosis. The improvement in mitochondrial dynamics and the NMDAR-CREB-BDNF pathway are vital mechanisms of DL0410 in promoting synaptic function and inhibiting neuronal apoptosis, and ultimately ameliorating cognitive impairments in SAMP8 mice.

BDNF-induced neurotrophic effect, and the NMDAR-CREB-BDNF pathway also provides the necessary conditions for mitochondrial dynamics in neurons. Here, all of our conclusions are deduced from the available facts and evidence. However, the key upstream molecule that improves mitochondrial dynamics and/or the NMDAR-CREB-BDNF pathway needs to be identified and verified to further support our conclusions.

In summary, DL0410 effectively ameliorated learning and memory deficits in 8-month-old SAMP8 mice after 8 weeks administration of DL0410. The improved mitochondrial dynamics and the NMDAR-CREB-BDNF pathway are vital mechanisms of DL0410 in improving memory in the SAMP8 mice. Therefore, DL0410 is a promising candidate for AD treatment and deserves more in vitro studies to define its mechanisms in the future.

## ACKNOWLEDGEMENTS

The study was supported by the National Great Science Technology Projects (2014ZX09507003-002), the Drug Innovation Major Project (No. 2018ZX09711001-003-002), the CAMS Initiative for Innovative Medicine (CAMS-IZM) (2016-IZM-3-007), the Beijing Natural Science Foundation (7192134, 7204303), and the National Natural Science Foundation of China (81673480).

## AUTHOR CONTRIBUTIONS

WWL, ALL, and GHD designed the experiment and revised the paper; WZ, BYZ, HJ, and LJX performed the experiments; WWL and WZ analyzed the data. All authors listed have made direct contributions to the work and approved it for publication.

## ADDITIONAL INFORMATION

**Competing interests:** The authors declare that the research was conducted in the absence of any commercial or financial relationships that could be construed as a potential conflict of interest.

## REFERENCES

1. Scheltens P, Blennow K, Breteler MMB, de Strooper B, Frisoni GB, Salloway S, et al. Alzheimer's disease. Lancet. 2016;388:505–17.
2. Lane CA, Hardy J, Schott JM. Alzheimer's disease. Eur J Neurol. 2018;25:59–70.
3. Alzheimer's Association. Alzheimer's disease facts and figures. Alzheimer's Dement. 2016;12:459–509.
4. Briggs R, Kennelly SP, O'Neill D. Drug treatments in Alzheimer's disease. Clin Med. 2016;16:247–53.
5. Fang JS, Li Y, Liu R, Pang XC, Li C, Yang RY, et al. Discovery of multitarget-directed ligands against Alzheimer's disease through systematic prediction of chemical–protein interactions. J Chem Inf Model. 2015;55:149–64.
6. Fang JS, Yang RY, Gao L, Zhou D, Yang SQ, Liu AL, et al. Predictions of BuChE inhibitors using support vector machine and Naive Bayesian classification techniques in drug discovery. J Chem Inf Model. 2013;53:3009–20.
7. Pang XC, Zhao Y, Song JK, Kang D, Wu S, Wang L, et al. Pharmacokinetics, excretion and metabolites analysis of DL0410, a dual-acting cholinesterase inhibitor and histamine3 receptor antagonist. Mol Med Rep. 2019;20:1103–12.
8. Lian WW, Fang JS, Xu LJ, Zhou W, Kang D, Xiong WD, et al. DL0410 ameliorates memory and cognitive impairments induced by scopolamine via increasing cholinergic neurotransmission in mice. Molecules. 2017;22:410. https://doi.org/10.3390/molecules22030410.
9. Lian WW, Jia H, Xu LJ, Zhou W, Kang D, Liu AL, et al. Multi-protection of DL0410 in ameliorating cognitive defects in *D*-galactose induced aging mice. Front Aging Neurosci. 2017;9:409. https://doi.org/10.3389/fnagi.2017.00409.
10. Zhou D, Zhou W, Song JK, Feng ZY, Yang RY, Wu S, et al. DL0410, a novel dual cholinesterase inhibitor, protects mouse brains against Abeta-induced neuronal damage via the Akt/JNK signaling pathway. Acta Pharmacol Sin. 2016;37:1401–12.
11. Yang RY, Zhao G, Wang DM, Pang XC, Wang SB, Fang JS, et al. DL0410 can reverse cognitive impairment, synaptic loss and reduce plaque load in APP/PS1 transgenic mice. Pharmacol Biochem Behav. 2015;139:15–26.
12. Zhou W, Lian WW, Yan R, Jia H, Xu LJ, Wang L, et al. DL0410 ameliorates cognitive deficits in APP/PS1 transgenic mice by promoting synaptic transmission and reducing neuronal loss. Acta Pharmacol Sin. 2020;41:599–611.
13. Karuppagounder V, Arumugam S, Babu SS, Palaniyandi SS, Watanabe K, Cooke JP, et al. The senescence accelerated mouse prone 8 (SAMP8): a novel murine model for cardiac aging. Ageing Res Rev. 2017;35:291–6.
14. Akiguchi I, Pallas M, Budka H, Akiyama H, Ueno M, Han J, et al. SAMP8 mice as a neuropathological model of accelerated brain aging and dementia: Toshio Takeda's legacy and future directions. Neuropathology. 2017;37:293–305.
15. Cheng XR, Zhou WX, Zhang YX. The behavioral, pathological and therapeutic features of the senescence-accelerated mouse prone 8 strain as an Alzheimer's disease animal model. Aging Res Rev. 2014;13:13–37.
16. Leonard JV, Schapira AH. Mitochondrial respiratory chain disorders II: neurodegenerative disorders and nuclear gene defects. Lancet. 2000;355:389–94.
17. Sinha K, Das J, Pal PB, Sil PC. Oxidative stress: the mitochondria-dependent and mitochondria-independent pathways of apoptosis. Arch Toxicol. 2013;87:1157–80.
18. Dai Z, Lu XY, Zhu WL, Liu XQ, Li BY, Song L, et al. Carnosine ameliorates age-related dementia via improving mitochondrial dysfunction in SAMP8 mice. Food Funct. 2020;11:2489–97.
19. Zhu WL, Zheng JY, Cai WW, Dai Z, Li BY, Xu TT, et al. Ligustilide improves aging-induced memory deficit by regulating mitochondrial related inflammation in SAMP8 mice. Aging. 2020;12:3175–89.
20. Gaskill BN, Karas AZ, Garner JP, Pritchett-Corning KR. Nest building as an indicator of health and welfare in laboratory mice. J Vis Exp. 2013;82:51012. https://doi.org/10.3791/51012.
21. Otabi H, Goto T, Okayama T, Kohari D, Toyoda A. Subchronic and mild social defeat stress alter mouse nest building behavior. Behav Process. 2016;122:21–5.
22. Greenberg GD, Huang LC, Spence SE, Schlumbohm JP, Metten P, Ozburn AR, et al. Nest building is a novel method for indexing severity of alcohol withdrawal in mice. Behav Brain Res. 2016;302:182–90.
23. Sheng B, Wang X, Su B, Lee HG, Casadesus G, Perry G, et al. Impaired mitochondrial biogenesis contributes to mitochondrial dysfunction in Alzheimer's disease. J Neurochem. 2012;120:419–29.
24. Rice AC, Keeney PM, Algarzae NK, Ladd AC, Thomas RR, Bennett JP Jr. Mitochondrial DNA copy numbers in pyramidal neurons are decreased and mitochondrial biogenesis transcriptome signaling is disrupted in Alzheimer's disease hippocampi. J Alzheimers Dis. 2014;40:319–30.
25. Dong W, Quo W, Wang F, Li C, Xie Y, Zheng X, et al. Electroacupuncture upregulates SIRT1-dependent PGC-1alpha expression in SAMP8 mice. Med Sci Monit. 2015;21:3356–62.
26. Eckert GP, Schiborr C, Hagl S, Abdel-Kader R, Muller WE, Rimbach G, et al. Curcumin prevents mitochondrial dysfunction in the brain of the senescence-accelerated mouse-prone 8. Neurochem Int. 2013;62:595–602.
27. Pedros I, Petrov D, Allgaier M, Sureda F, Barroso E, Beas-Zarate C, et al. Early alterations in energy metabolism in the hippocampus of APPswe/PS1dE9 mouse model of Alzheimer's disease. Biochim Biophys Acta. 2014;1842:1556–66.
28. Chan DC. Mitochondrial fusion and fission in mammals. Annu Rev Cell Dev Biol. 2006;22:79–99.
29. Zhang W, Gu GJ, Shen X, Zhang Q, Wang GM, Wang PJ. Neural stem cell transplantation enhances mitochondrial biogenesis in a transgenic mouse model of Alzheimer's disease-like pathology. Neurobiol Aging. 2015;36:1282–92.
30. Manczak M, Reddy PH. Abnormal interaction between the mitochondrial fission protein Drp1 and hyperphosphorylated tau in Alzheimer's disease neurons: implications for mitochondrial dysfunction and neuronal damage. Hum Mol Genet. 2012;21:2538–47.
31. Picca A, Pesce V, Sirago G, Fracasso F, Leeuwenburgh C, Lezza AMS. "What makes some rats live so long?" The mitochondrial contribution to longevity through balance of mitochondrial dynamics and mtDNA content. Exp Gerontol. 2016;85:33–40.
32. Reddy PH, Reddy TP, Manczak M, Calkins MJ, Shirendeb U, Mao P. Dynamin-related protein 1 and mitochondrial fragmentation in neurodegenerative diseases. Brain Res Rev. 2011;67:103–18.
33. Yang X, Yao C, Tian T, Li X, Yan H, Wu J, et al. Synaptic mechanism in Alzheimer's disease: a selective degeneration of an excitatory synaptic pathway in the CA1 hippocampus that controls spatial learning and memory in Alzheimer's disease. Mol Psychiatry. 2018;23:167.
34. Lista S, Hampel H. Synaptic degeneration and neurogranin in the pathophysiology of Alzheimer's disease. Expert Rev Neurother. 2017;17:47–57.
35. Gong Y, Lippa CF. Review: disruption of the postsynaptic density in Alzheimer's disease and other neurodegenerative dementias. Am J Alzheimers Dis Other Demen. 2010;25:547–55.
36. Love S, Siew LK, Dawbarn D, Wilcock GK, Ben-Shlomo Y, Allen SJ. Premorbid effects of APOE on synaptic proteins in human temporal neocortex. Neurobiol Aging 2006;27:797–803.
37. Gerenu G, Liu K, Chojnacki JE, Saathoff JM, Martinez Martin P, Perry G. et al. Curcumin/melatonin hybrid 5-(4-hydroxy-phenyl)-3-oxo-pentanoic acid [2-(5-methoxy-1H-indol-3-yl)-ethyl]-amide ameliorates AD-like pathology in the APP/PS1 mouse model. ACS Chem Neurosci.2015;6:1393–9.
38. Zhang Y, Huang LJ, Shi S, Xu SF, Wang XL, Peng Y. L-3-*n*-butylphthalide rescues hippocampal synaptic failure and attenuates neuropathology in aged APP/PS1 mouse model of Alzheimer's disease. CNS Neurosci Ther. 2016;22:979–87.

39. Ma J, Wang J, Lv C, Pang J, Han B, Wang M, et al. The role of hippocampal structural synaptic plasticity in repetitive transcranial magnetic stimulation to improve cognitive function in male SAMP8 mice. Cell Physiol Biochem. 2017;41:137–44.
40. Zhu L, Yang L, Zhao X, Liu D, Guo X, Liu P, et al. Xanthoceraside modulates NR2B-containing NMDA receptors at synapses and rescues learning-memory deficits in APP/PS1 transgenic mice. Psychopharmacol (Berl). 2018;235:337–49.
41. Giese KP, Fedorov NB, Filipkowski RK, Silva AJ. Autophosphorylation at Thr286 of the alpha calcium-calmodulin kinase II in LTP and learning. Science. 1998;279:870–3.
42. Moriguchi S, Kita S, Yabuki Y, Inagaki R, Izumi H, Sasaki Y, et al. Reduced CaM kinase II and CaM kinase IV activities underlie cognitive deficits in NCKX2 heterozygous mice. Mol Neurobiol. 2018;55:3889–900.
43. Barco A, Alarcon JM, Kandel ER. Expression of constitutively active CREB protein facilitates the late phase of long-term potentiation by enhancing synaptic capture. Cell. 2002;108:689–703.
44. Leal G, Afonso PM, Salazar IL, Duarte CB. Regulation of hippocampal synaptic plasticity by BDNF. Brain Res. 2015;1621:82–101.
45. Leal G, Bramham CR, Duarte CB. BDNF and hippocampal synaptic plasticity. Vitam Horm. 2017;104:153–95.
46. Kuczewski N, Porcher C, Lessmann V, Medina I, Gaiarsa JL. Activity-dependent dendritic release of BDNF and biological consequences. Mol Neurobiol. 2009;39:37–49.
47. Panja D, Bramham CR. BDNF mechanisms in late LTP formation: a synthesis and breakdown. Neuropharmacology. 2014;76:664–76.
48. Leal G, Comprido D, Duarte CB. BDNF-induced local protein synthesis and synaptic plasticity. Neuropharmacology. 2014;76:639–56.
49. Braun DJ, Kalinin S, Feinstein DL. Conditional depletion of hippocampal brain-derived neurotrophic factor exacerbates neuropathology in a mouse model of Alzheimer's Disease. ASN Neuro. 2017;9:1759091417696161.
50. Lu Y, Christian K, Lu B. BDNF: a key regulator for protein synthesis-dependent LTP and long-term memory? Neurobiol Learn Mem. 2008;89:312–23.
51. Patterson SL, Abel T, Deuel TA, Martin KC, Rose JC, Kandel ER. Recombinant BDNF rescues deficits in basal synaptic transmission and hippocampal LTP in BDNF knockout mice. Neuron. 1996;16:1137–45.
52. Wang CC, Guo Y, Zhou MM, Xue CH, Chang YG, Zhang TT, et al. Comparative studies of DHA-enriched phosphatidylcholine and recombination of DHA-ethyl ester with egg phosphatidylcholine on ameliorating memory and cognitive deficiency in SAMP8 mice. Food Funct. 2019;10:938–50.
53. Lu Y, Ji Y, Ganesan S, Schloesser R, Martinowich K, Sun M, et al. TrkB as a potential synaptic and behavioral tag. J Neurosci. 2011;31:11762–71.
54. Minichiello L, Korte M, Wolfer D, Kuhn R, Unsicker K, Cestari V, et al. Essential role for TrkB receptors in hippocampus-mediated learning. Neuron. 1999;24:401–14.
55. Su D, Zhao J, Hu S, Guan L, Li Q, Shi C, et al. GSK3beta and MCL-1 mediate cardiomyocyte apoptosis in response to high glucose. Histochem Cell Biol. 2019;152:217–25.
56. Li Q, Che HX, Wang CC, Zhang LY, Ding L, Xue CH, et al. Cerebrosides from sea cucumber improved $A\beta_{(1-42)}$-induced cognitive deficiency in a rat model of Alzheimer's disease. Mol Nutr Food Res. 2019;63:e1800707.
57. Aouacheria A, Baghdiguian S, Lamb HM, Huska JD, Pineda FJ, Hardwick JM. Connecting mitochondrial dynamics and life-or-death events via Bcl-2 family proteins. Neurochem Int. 2017;109:141–61.
58. D'Orsi B, Mateyka J, Prehn JHM. Control of mitochondrial physiology and cell death by the Bcl-2 family proteins Bax and Bok. Neurochem Int. 2017;109:162–70.
59. Wang CC, Wang D, Zhang TT, Yanagita T, Xue CH, Chang YG, et al. A comparative study about EPA-PL and EPA-EE on ameliorating behavioral deficits in MPTP-induced mice with Parkinson's disease by suppressing oxidative stress and apoptosis. J Funct Food. 2018;50:8–17.
60. Wang CC, Wang D, Xu J, Yanagita T, Xue C, Zhang TT, et al. DHA enriched phospholipids with different polar groups (PC and PS) had different improvements on MPTP-induced mice with Parkinson's disease. J Funct Food. 2018;45:417–26.